

## Dynamic response for electromechanical integrated toroidal drive to electric excitation

Lizhong Xu<sup>†</sup> and Xiuhong Hao

Mechanical Engineering Institute, Yanshan University, Qinhuangdao 066004, China

(Received March 28, 2006, Accepted February 22, 2007)

**Abstract.** In this paper, the equivalent exciting force caused by electric excitation is derived. By dividing load and displacement vectors into mean values and time-varying ones, the dynamic equations of the system are transformed into linear ones for time-varying portion of the displacements. The analytical equations of the forced time responses of the drive system to electric excitations are obtained. Using the Laplace transformation, the transfer function of the drive system is obtained. These equations are used to analyze the time and frequency responses of the drive system to the electric excitation. It is known that electric excitation can cause forced responses of the drive system, the total dynamic responses are decided by three phase exciting voltages, exciting frequency and natural frequencies of the drive system, and the drive parameters have obvious influence on the time and frequency responses.

**Keywords:** toroidal drive; electromechanical integrated; dynamic response; electric excitation.

---

### 1. Introduction

Toroidal drive can transmit large torque in a very small size and is suitable for technical fields such as aviation, space flight, and so on Kuehnle (1966, 1981). In Kuehnle (1998, 1999), the new type of the toroidal drive was proposed and a method of assembling the drive was disclosed. In Lizhong (2004), Lizhong *et al.* (2004), Lizhong and Zhen (2003) investigated operating efficiency, mesh theory and contact stress of the drive. In Yao *et al.* (2004, 2005), a new manufacturing principle of the stator was investigated. In Yao *et al.* (2005, 2006), meshing characteristics with respect to different meshing rollers of the toroidal drive were discussed. In Yao *et al.* (2006), the error and compensation for toroidal drive were analyzed.

As electrical and control techniques are utilized in mechanical engineering field, generalized composite drives become advancing edge of the mechanical science. The electromagnetic harmonic drive (Da Lio *et al.* 1994, Shang and You 1997) and piezoelectric harmonic one (Barth 2005) are active drives in which the meshing forces between flexible gear and rigid gear are controlled by electromagnetic force or piezoelectric force, and drive and power are integrated. The permanent magnetic gearing (Rasmussen *et al.* 2003, Atallah *et al.* 2004, Okano *et al.* 2002) is a passive drive in which mechanical elements and magnetic elements are integrated. The main advantage of the permanent magnetic gearing is meshes without contact.

---

<sup>†</sup> Ph.D., E-mail: Xlz@ysu.edu.cn

Based on the toroidal drive, the authors presented a kind of active generalized composite drive: electromechanical integrated toroidal drive. In the drive, the toroidal drive, power and control are integrated (Xu and Huang 2005).

The drive consists of four basic elements, Fig. 1: (a) the central worm; (b) radially positioned planets; (c) a toroidal shaped stator; and (d) a rotor, which forms the central output shaft upon which the planets are mounted. The central worm is fixed and the coils are mounted in helical grooves of its surface. The planets have permanent magnets instead of teeth. The N and S polar permanent magnets are mounted alternately on a planet. The stator has helical permanent magnets instead of helical teeth. In the same manner as planet, The N and S polar helical permanent magnets are mounted alternately on the stator.

If a specific parameter relation is realized, N pole of one element will correspond to the S pole of the other one all along. The attractive forces between N and S pole of the different elements are the driving forces and the meshes without contact are realized. When the alternate current is connected to the coils of the worm, a toroidal circular field is formed. It drives several planets to rotate about their own axes. By means of magnetic forces between teeth of the planet and stator, the rotor is driven to rotate about its own axis. Thus, a power of low speed and large torque is obtained.

When compared with the toroidal drive, the new drive is easy to produce, without wear, and does not need lubrication. It can be substituted for a servo system to simplify the structure of the existing electromechanical systems. Besides the aforementioned fields that require compactness, the drive can also be used in fields such as robots, where accurate control is required.

The operating behavior of the drive is influenced by fluctuation of the electric parameters. Therefore, the dynamic responses of the drive system to electric excitation should be investigated.

In this paper, based on electromechanical coupled dynamic equations for the drive system, the

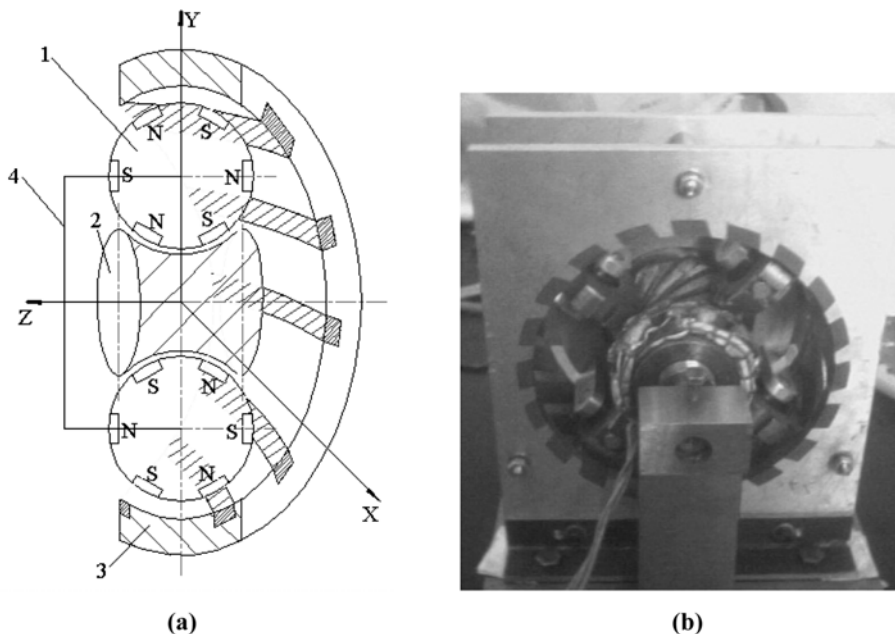


Fig. 1 The electromechanical integrated toroidal drive  
(a) Diagram of the drive (1. Planet 2. Worm 3. Stator 4. Rotor), (b) Model machine of the drive

dynamic response of the drive system to electric excitation is investigated. Based on the analysis of the electromechanical coupled forces, the equivalent exciting force caused by electric excitation is derived. By dividing load and displacement vectors into mean values and time-varying ones, the dynamic equations of the drive system are transformed into the linear ones for time-varying portion of the displacements. The analytical equations of the forced time responses for the drive system to electric excitations are obtained. Using the Laplace transformation, the transfer function of the drive system is given. These equations are used to analyze the forced time and frequency responses for the drive system to the electric excitation. Changes of the time and frequency response along with main parameters of the drive system are also obtained. It is known that electric excitation can cause forced responses of the drive system, the total dynamic responses are decided by three phase exciting voltages, exciting frequency and natural frequencies of the drive system, drive parameters have obvious influence on the time and frequency responses, and it is because mesh stiffness and equivalent exciting force of the drive system are influenced by these parameters. These results can be used to predict the noise and dynamic load and are useful in maximizing the power density of the drive and reducing noise radiation.

## 2. The equivalent exciting force

Space phase relation of the worm coils is shown in Fig. 2. In Fig. 2, the lines AA, BB and CC represent three phase worm coils, respectively. The points 1,2,3,4 are four planet teeth, respectively. The symbol  $\phi_v$  denotes face width angle of the worm. Then, in the transverse plane of the planet, the phase angle of the phase- $i$  is

$$\phi_i = \frac{i-1}{n_p} \frac{\phi_v}{p} \quad (i = 1 \text{ to } n_p)$$

where  $n_p$  is phase number of the worm coils ( $n_p = 3$ ),  $p$  is number of the pole-pairs, here subscript  $i$  represents the phase.

Let position angle  $\theta = 0$  of the planet when tooth of the planet is aligned completely with phase-1 coil. Inductances of the every phase can be calculated as below

### Self-inductances:

$$L_{ii} = L_0 + L_1 \cos\left(z_1 \theta - (i-1) \frac{\phi_v}{pn_p}\right) \quad (i = 1 \text{ to } n_p)$$

where  $L_{ii}$  is self-inductance of the  $i$ th phase coils,  $L_0$  is average inductance,  $L_1$  is the first order harmonic component of the inductance. Here, the subscript 0 means average value, the subscript 1 means the first order harmonic component.

### mutual-inductances between adjacent phases:

$$L_{i-1,i} = L_{01} + L_1 \cos\left(z_1 \theta - (2i-3) \frac{\phi_v}{2pn_p}\right) \quad (i = 2 \text{ to } n_p)$$

where  $L_{01}$  is average mutual-inductance between the adjacent two phase coils, the subscript 01 means the adjacent two phases.

**mutual-inductances between two spacing phases:**

$$L_{i-2,i} = L_{02} + L_1 \cos\left(z_1 \theta - (2i-4) \frac{\phi_v}{2pn_p}\right) \quad (i = 3 \text{ to } n_p)$$

where  $L_{02}$  is average mutual-inductance between the spacing two phases coils, the subscript 02 represents the spacing two phases, here  $L_{0i} = L_0 \cos \frac{i\phi_v}{pn_p}$  ( $i = 1$  to  $n_p$ ),  $z_1$  is tooth number of the planet.

The magnetic linkage  $\lambda_i$  of the worm coils can be calculated as follows

$$\lambda_i = \sum_{j=1}^n L_{ij} I_j \tag{1}$$

where  $I_i$  is the current in the  $i$ th phase worm coils,  $L_{ij}$  is the mutual-inductance of the coils, the subscript  $j$  represents the phase different from the phase  $i$ .

The magnetic energy stored in the electric system is

$$W = \frac{1}{2} \sum_{i=1}^n \lambda_i I_i \tag{2}$$

Symbols  $d\zeta$  and  $d\theta$  denote relative displacement and relative rotating angle between magnet poles of the different elements, respectively, and then  $d\zeta = R d\theta$ . The electromagnetic force between magnet poles is calculated as follows

$$F = -\frac{\partial W}{\partial \zeta} = -\frac{1}{R} \frac{\partial W}{\partial \theta} \tag{3}$$

Substituting Eqs. (1) and (2) into (3), the electromechanical coupled force between a tooth of the planet and worm is given as

$$F_{wp} = -\frac{1}{R} \frac{\partial W}{\partial \theta} = -\frac{1}{R} \sum_{j=1}^n \sum_{i=1}^n \frac{dL_{ij}}{d\theta} I_i I_j \tag{4}$$

where the subscript  $w$  represents worm, the subscript  $p$  represents planet.

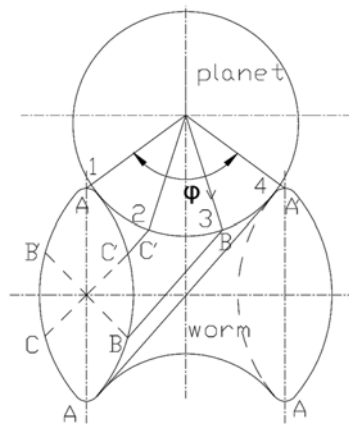


Fig. 2 Space phase relation of the worm coils

Let  $F_e(t)$  denote equivalent electric exciting force,  $\Delta F_{wp}$  denote increment of the magnetic meshing force between a planet and worm, then

$$F_e(t) = -\frac{1}{2R} \sum_{j=1}^n \sum_{i=1}^n \left[ \left( \frac{\partial L_{ij}}{\partial \theta} \right)_{\theta=\theta_0} I_i \delta I_j + \left( \frac{\partial L_{ij}}{\partial \theta} \right)_{\theta=\theta_0} I_j \delta I_i \right] \quad (5)$$

$$\Delta F_{wp} = -\frac{1}{2R} \sum_{i=1}^n \sum_{j=1}^n \left( \frac{\partial^2 L_{ij}}{\partial \theta^2} \right)_{\theta=\theta_0} I_i I_j \delta \theta \quad (6)$$

As three phase currents are connected to coils of the worm, Eq. (5) can be changed into following form

$$\begin{aligned} F_e(t) = & -\frac{1}{2} \left[ \left( \frac{\partial L_{11}}{\partial \theta} \right)_{\theta=\theta_0} I_1 \delta I_1 + \left( \frac{\partial L_{12}}{\partial \theta} \right)_{\theta=\theta_0} I_1 \delta I_2 + \left( \frac{\partial L_{13}}{\partial \theta} \right)_{\theta=\theta_0} I_1 \delta I_3 + \left( \frac{\partial L_{21}}{\partial \theta} \right)_{\theta=\theta_0} I_2 \delta I_1 \right. \\ & + \left( \frac{\partial L_{22}}{\partial \theta} \right)_{\theta=\theta_0} I_2 \delta I_2 + \left( \frac{\partial L_{23}}{\partial \theta} \right)_{\theta=\theta_0} I_2 \delta I_3 + \left( \frac{\partial L_{31}}{\partial \theta} \right)_{\theta=\theta_0} I_3 \delta I_1 + \left( \frac{\partial L_{32}}{\partial \theta} \right)_{\theta=\theta_0} I_3 \delta I_2 + \left( \frac{\partial L_{33}}{\partial \theta} \right)_{\theta=\theta_0} I_3 \delta I_3 \\ & + \left( \frac{\partial L_{11}}{\partial \theta} \right)_{\theta=\theta_0} I_1 \delta I_1 + \left( \frac{\partial L_{21}}{\partial \theta} \right)_{\theta=\theta_0} I_2 \delta I_1 + \left( \frac{\partial L_{31}}{\partial \theta} \right)_{\theta=\theta_0} I_3 \delta I_1 + \left( \frac{\partial L_{12}}{\partial \theta} \right)_{\theta=\theta_0} I_1 \delta I_2 + \left( \frac{\partial L_{22}}{\partial \theta} \right)_{\theta=\theta_0} I_2 \delta I_2 \\ & \left. + \left( \frac{\partial L_{32}}{\partial \theta} \right)_{\theta=\theta_0} I_3 \delta I_2 + \left( \frac{\partial L_{13}}{\partial \theta} \right)_{\theta=\theta_0} I_1 \delta I_3 + \left( \frac{\partial L_{23}}{\partial \theta} \right)_{\theta=\theta_0} I_2 \delta I_3 + \left( \frac{\partial L_{33}}{\partial \theta} \right)_{\theta=\theta_0} I_3 \delta I_3 \right] \quad (7) \end{aligned}$$

Three phase electric excitation vector is given as below

$$\Delta \mathbf{v}(t) = \left[ v \sin(\omega_e t) \quad v \sin\left(\omega_e t - \frac{\pi}{3}\right) \quad v \sin\left(\omega_e t - \frac{2\pi}{3}\right) \right]^T \quad (8)$$

where  $v$  is the amplitude of the exciting voltage applied to coils,  $\omega_e$  is the frequency of the exciting voltage applied to coils.

When only the first phase voltage excitation is considered, substituting Eq. (8) into (7), the equivalent exciting force is

$$F_{e1}(t) = \frac{I z_1 L_1}{R} \left[ \sin(z_1 \theta) + \sin\left(z_1 \theta - \frac{\phi_v}{2n_p}\right) + \sin\left(z_1 \theta - \frac{\phi_v}{n_p}\right) \right] \frac{v}{r_\Omega} \sin(\omega_e t) \quad (9)$$

where  $r_\Omega$  is resistance of each phase worm coils,  $I$  is effective value of the current,  $I = I_1 = I_2 = I_3$ .

When only the second phase voltage excitation is considered, the equivalent exciting force is

$$F_{e2}(t) = \frac{I z_1 L_1}{R} \left[ \sin(z_1 \theta) + \sin\left(z_1 \theta - \frac{\phi_v}{2n_p}\right) + \sin\left(z_1 \theta - \frac{\phi_v}{n_p}\right) \right] \frac{v}{r_\Omega} \sin\left(\omega_e t + \frac{\pi}{3}\right) \quad (10)$$

When only the third phase voltage excitation is considered, the equivalent exciting force is

$$F_{e3}(t) = \frac{I z_1 L_1}{R} \left[ \sin(z_1 \theta) + \sin\left(z_1 \theta - \frac{\phi_v}{2n_p}\right) + \sin\left(z_1 \theta - \frac{\phi_v}{n_p}\right) \right] \frac{v}{r_\Omega} \sin\left(\omega_e t + \frac{2\pi}{3}\right) \quad (11)$$

### 3. The dynamic response of the drive system to electric excitations

The dynamic equations for the electromechanical integrated toroidal drive is derived as below

$$\mathbf{M}\ddot{\mathbf{X}} + \mathbf{C}\dot{\mathbf{X}} + \mathbf{K}\mathbf{X} = \mathbf{F} \tag{12}$$

where  $\mathbf{X}$  and  $\mathbf{F}$  are displacement and load vectors, respectively

$$\mathbf{X} = \{ \mathbf{q}_1 \dots \dots \mathbf{q}_m \ u_r \}^T$$

$$\mathbf{F} = \{ \mathbf{0} \dots \dots \mathbf{0} \ -T_r/r_r \}^T$$

$\mathbf{M}$ ,  $\mathbf{C}$  and  $\mathbf{K}$  are mass, damp and stiffness matrix, respectively, the subscript  $r$  represents rotor.

$$\mathbf{M} = \text{diag}[\mathbf{m}_1 \dots \dots \mathbf{m}_m \ M_r]$$

$$\mathbf{K} = \begin{bmatrix} \mathbf{k}_{wp1} + \mathbf{k}_{sp1} + \mathbf{k}_{cp1} & \dots & \mathbf{0} & \dots & \mathbf{0} & \mathbf{k}_{c1} \\ & \ddots & \vdots & \dots & \vdots & \vdots \\ & & \mathbf{k}_{wpi} + \mathbf{k}_{spi} + \mathbf{k}_{cpi} & \dots & \vdots & \mathbf{k}_{ci} \\ & & & \ddots & \vdots & \vdots \\ & & & & \mathbf{k}_{wpm} + \mathbf{k}_{spm} + \mathbf{k}_{cpm} & \mathbf{k}_{cm} \\ & & & & & \sum_{i=1}^m k_{czi} \end{bmatrix}$$

*symmetric*

here,  $\mathbf{k}_{wpi} = k_{wpi} \begin{bmatrix} \sin^2 \gamma_{wpi} & 0 & -\cos \gamma_{wpi} \sin \gamma_{wpi} \\ 0 & 0 & 0 \\ -\cos \gamma_{wpi} \sin \gamma_{wpi} & 0 & \cos^2 \gamma_{wpi} \end{bmatrix}$ ,  $\mathbf{k}_{spi} = k_{spi} \begin{bmatrix} \cos^2 \gamma_{spi} & 0 & \sin \gamma_{spi} \cos \gamma_{spi} \\ 0 & 0 & 0 \\ \sin \gamma_{spi} \cos \gamma_{spi} & 0 & \sin^2 \gamma_{spi} \end{bmatrix}$

$$\mathbf{k}_{cpi} = \begin{bmatrix} 0 & 0 & 0 \\ 0 & k_{cxi} & 0 \\ 0 & 0 & k_{czi} \end{bmatrix} \text{ and } \mathbf{k}_{ci} = \{ 0 \ 0 \ -k_{czi} \}^T. \ k_{wpi} \text{ and } k_{spi} \text{ are mesh stiffness between planet-}i \text{ and}$$

worm or stator, respectively;  $k_{czi}$  and  $k_{cxi}$  are planet support stiffness in axial and radial directions, respectively.

For the sake of convenience, the rotations are replaced by their corresponding translational mesh displacements as  $u_j = r_j \theta_j$ ,  $j = 1, \dots, n, r$ . Here,  $m$  is planet number,  $\theta_j$  is the rotation of planet or rotor,  $r_j$  is the rolling circle radius for planet and the radius of the circle passing through planet centers for the rotor. A displacement vector  $\mathbf{q}_j$  and a mass matrix  $\mathbf{m}_j$  are defined for each planet  $j$  as  $\mathbf{q}_j = [u_j \ x_j \ z_j]^T$  and  $\mathbf{m}_j = \text{Diag}[J_j/r_j^2 \ m_j \ m_j]$ . Here,  $J_j$  and  $m_j$  are polar mass moment of inertia and mass for planet  $j$ , respectively.  $M_r (M_r = J_r/r_r^2)$  is equivalent mass of rotor corresponding to its displacement  $u_r$ . Here, subscript  $j$  means the  $j$ th planet.

The total load of the drive system consists of the static load and the dynamic load. Hence, the load vector is

$$\mathbf{F} = \bar{\mathbf{F}} + \Delta\mathbf{F} \tag{13}$$

where  $\bar{\mathbf{F}}$  and  $\Delta\mathbf{F}$  are the static load vector and the dynamic load vector, respectively

$$\Delta \mathbf{F} = \{ \mathbf{F}_e \dots \dots \mathbf{F}_e \mathbf{0} \}^T \text{ and } \mathbf{F}_e = \{ \sin \gamma_{wpi} F_e(t) \ 0 \ \cos \gamma_{wpi} F_e(t) \}^T$$

$\gamma_{wpi}$  and  $\gamma_{spi}$  are the lead angles at contact point between planet- $i$  and worm or stator, respectively. The subscript  $pi$  means  $i$ th planet.

Then, the total forced displacement of the each component consists of the static displacement and the dynamic displacement as well. Hence, the displacement vector is

$$\mathbf{X} = \bar{\mathbf{X}} + \Delta \mathbf{X} \tag{14}$$

where  $\bar{\mathbf{X}}$  and  $\Delta \mathbf{X}$  are the static displacement vector and the dynamic displacement vector, respectively,  $\Delta \mathbf{X} = \{ \Delta \mathbf{q}_1 \dots \dots \Delta \mathbf{q}_m \ \Delta u_r \}^T$  and  $\Delta \mathbf{q}_j = [ \Delta u_j \ \Delta x_j \ \Delta z_j ]^T$ , the subscript  $j$  means the  $j$ th planet.

Eqs. (13) and (14) are substituted into Eq. (12), under condition that nonlinear terms are neglected, the linear dynamic equations of the drive system are obtained

$$\mathbf{M} \Delta \ddot{\mathbf{X}} + \mathbf{C} \Delta \dot{\mathbf{X}} + \mathbf{K} \Delta \mathbf{X} = \Delta \mathbf{F} \tag{15}$$

The Eq. (15) decides a set of equations that are coupled with each other. For simplicity purposes, the equations should be transmitted into equations independent of each other. Then, Eq. (15) can be changed into the following form

$$\mathbf{M}_r \Delta \ddot{\mathbf{X}}_r + \mathbf{C}_r \Delta \dot{\mathbf{X}}_r + \mathbf{K}_r \Delta \mathbf{X}_r = \Delta \mathbf{F}_r \tag{16}$$

where  $\mathbf{M}_r$ ,  $\mathbf{C}_r$  and  $\mathbf{K}_r$  are the diagonal mass, damping and stiffness matrices, respectively.  $\Delta \mathbf{F}_r$  and  $\Delta \mathbf{X}_r$  are the transmitted exciting force and dynamic displacement vectors, respectively. Matrices  $\mathbf{M}_r$ ,  $\mathbf{C}_r$  and  $\mathbf{K}_r$ , vectors  $\Delta \mathbf{F}_r$  and  $\Delta \mathbf{X}_r$  are given as

$$\mathbf{M}_r = \mathbf{A}_r^T \mathbf{M} \mathbf{A}_r, \ \mathbf{C}_r = \mathbf{A}_r^T \mathbf{C} \mathbf{A}_r, \ \mathbf{K}_r = \mathbf{A}_r^T \mathbf{K} \mathbf{A}_r, \ \Delta \mathbf{F}_r = \mathbf{A}_r^T \Delta \mathbf{F}, \ \Delta \mathbf{X}_r = \mathbf{A}_r^T \Delta \mathbf{X}$$

Here  $\mathbf{A}_r$  is the mode matrix of the Eq. (15).

Eq. (16) can be replaced by following equation

$$\ddot{x}_{Nr} + 2 \gamma_r \omega_r \dot{x}_{Nr} + \omega_r^2 x_{Nr} = \Delta F_{Nr}(t) \quad (r = 1 \text{ to } 3m + 1) \tag{17}$$

where  $\omega_r = \sqrt{K_r/M_r}$ ,  $\gamma_r = c_{Nr}/2 \omega_r$ ,  $\Delta F_{Nr}(t)$  is the  $r$ th regular exciting force,  $M_r$  and  $K_r$  are the  $r$ th transmitted mass and transmitted stiffness, respectively.  $m$  is the planet number.

When initial conditions  $\{ \dot{x}_N \}_{t=0} = 0$ ,  $\{ x_N \}_{t=0} = 0$  are given, under condition that the  $i$ th phase voltage excitation is considered, the time response of the  $r$ th regular coordinate  $x_{Nr}$  is

$$x_{Nr} = \frac{\Delta F_{Nr} e^{-\gamma \omega_r t}}{\omega_r'} \left[ \sin \omega_r' t \int_0^t \sin \left( \omega t' + \frac{(i-1)\pi}{3} \right) \cos \omega_r' t' e^{\gamma_r \omega_r' t'} dt' \right. \\ \left. - \cos \omega_r' t \int_0^t \sin \left( \omega t' + \frac{(i-1)\pi}{3} \right) e^{\gamma_r \omega_r' t'} \sin \omega_r' t' dt' \right] \quad (i = 1 \text{ to } 3) \tag{18}$$

where  $\omega_r' = \omega_r \sqrt{1 - \gamma^2}$ ,  $\Delta F_{Nr}$  is the amplitude of the  $r$ th regular exciting force.

From Eq. (18), the following equation can be obtained

$$\begin{aligned}
 x_{Nr} = \frac{\Delta F_{Nr}}{\omega_r'} & \left\{ e^{-\gamma\omega_r t} \left[ \frac{\left( \omega + \omega_r' + \frac{(i-1)\pi}{3} \right) \sin \omega_r' t + \gamma\omega_r \cos \omega_r' t}{(\gamma\omega_r)^2 + \left( \omega + \omega_r' + \frac{(i-1)\pi}{3} \right)^2} \right. \right. \\
 & \left. \left. + \frac{\left( \omega - \omega_r' + \frac{(i-1)\pi}{3} \right) \sin \omega_r' t - \gamma\omega_r \cos \omega_r' t}{(\gamma\omega_r)^2 + \left( \omega - \omega_r' + \frac{(i-1)\pi}{3} \right)^2} \right] \right. \quad (i = 1 \text{ to } 3) \\
 & - \frac{\left( \omega + \omega_r' + \frac{(i-1)\pi}{3} \right) \sin \left( 2\omega_r' + \omega + \frac{(i-1)\pi}{3} \right) t + \gamma\omega_r \cos \left( 2\omega_r' + \omega + \frac{(i-1)\pi}{3} \right) t}{(\gamma\omega_r)^2 + \left( \omega + \omega_r' + \frac{(i-1)\pi}{3} \right)^2} \\
 & \left. + \frac{\left( \omega - \omega_r' + \frac{(i-1)\pi}{3} \right) \sin \left( 2\omega_r' - \omega + \frac{(i-1)\pi}{3} \right) t + \gamma\omega_r \cos \left( 2\omega_r' - \omega + \frac{(i-1)\pi}{3} \right) t}{(\gamma\omega_r)^2 + \left( \omega - \omega_r' + \frac{(i-1)\pi}{3} \right)^2} \right\} \quad (19)
 \end{aligned}$$

Using the Laplace transformation for Eq. (16), the frequency response of the drive system is given

$$\Delta \mathbf{X}_r(s) = \frac{\Delta \mathbf{F}_r(s)}{\mathbf{M}_r s^2 + \mathbf{C}_r s + \mathbf{K}_r} \quad (20)$$

where  $\Delta \mathbf{F}_r(s) = \mathbf{A}_r^T \Delta \mathbf{F}(s)$ ,  $\Delta \mathbf{F}(s) = \{ \mathbf{F}_e(s) \dots \mathbf{F}_e(s) \mathbf{0} \}^T$

$$\mathbf{F}_e(s) = \{ \sin \gamma_{wpi} F_e(s) \quad 0 \quad \cos \gamma_{wpi} F_e(s) \}^T$$

$$F_e(s) = \left[ \sin(z_1 \theta) + \sin \left( z_1 \theta - \frac{\phi_v}{2n_p} \right) + \sin \left( z_1 \theta - \frac{\phi_v}{n_p} \right) \right] \frac{I z_1 L_1 v}{R} \frac{\omega_e}{r_\Omega \omega_e^2 - s^2}$$

Then, the real time and frequency responses of the drive system can be calculated as below

$$\Delta \mathbf{X} = \mathbf{A}_r \Delta \mathbf{X}_r \quad (21)$$

## 4. Results and discussions

### 4.1 Time response

From Eq. (12), let damping and load equal zero, the undamped equations of free vibration for the drive are given as

$$\mathbf{M} \ddot{\mathbf{X}} + \mathbf{K} \mathbf{X} = \mathbf{0} \quad (22)$$

Table 1 Parameters of the example system

$a/R$	$i_{sp}$	$i_{vp}$	$z_1$	$\phi_v(^{\circ})$	$m$	$nI(A)$	$L_0(H)$	$L_1(H)$	$r_{\Omega}(\Omega)$
2	0.25	8	8	80	3	45	$10^{-3}$	$10^{-3}$	10

Table 2 Natural frequencies of mechanical system for the drive (rad/s)

$r$	1	2	3	4	5	6	7	8	9	10
$\omega_r$	303	524	524	584	1686	1686	1919	2132	2132	2132

The parameters of the numerical example are shown in Table 1. The parameters are substituted into equations of the mass and stiffness matrix, and then the mass and stiffness matrix are substituted into Eq. (22), the natural frequencies of mechanical system for the drive system can be obtained as shown in Table 2.

Based on the natural frequencies, the mode matrix can be obtained as below

$$A = \begin{bmatrix} 0.0959 & 0.1276 & -1.0000 & -1.0000 & -1.0000 & -0.5000 & 0.0638 & 0 & 0 & 0 \\ 0 & 0 & 0 & 0 & 0 & 0 & 0 & 1.0000 & 0 & 0 \\ 1.0000 & 1.0000 & 0.06242 & -0.1685 & 0.0638 & 0.0319 & 0.50000 & 0 & 0 & 0 \\ 0.0959 & -0.0638 & -1.0000 & -1.0000 & 0.5000 & 1.0000 & 0.0638 & 0 & 0 & 0 \\ 0 & 0 & 0 & 0 & 0 & 0 & 0 & 0 & 1.0000 & 0 \\ 1.0000 & -0.5000 & 0.6242 & -1.1685 & -0.0319 & -0.0638 & 0.5000 & 0 & 0 & 0 \\ 0.0959 & -0.0638 & -1.0000 & -1.0000 & 0.5000 & -0.5000 & -0.1276 & 0 & 0 & 0 \\ 0 & 0 & 0 & 0 & 0 & 0 & 0 & 0 & 0 & 1.0000 \\ 1.0000 & -0.5000 & 0.6242 & -0.1685 & -0.0319 & 0.0319 & -1.000 & 0 & 0 & 0 \\ -0.3728 & 0.0000 & 0.6801 & -0.2555 & 0.0000 & 0.0000 & 0.0000 & 0 & 0 & 0 \end{bmatrix} \quad (23)$$

In matrix  $A$ , the first, third and fourth columns represent a 7-DOF vibration, respectively, in which the last term shows rotating vibration of the rotor. So these modes are named rotational mode. The second, fifth, sixth and seventh columns represent a 6-DOF vibration, respectively, in which the last term is zero and the rotating vibration of the rotor does not occur. As only vibrations of the planets occur and these modes are named planet mode. The eighth, ninth and tenth columns represent a 1-DOF vibration, respectively, in which only one term does not equal zero. As only the  $x_i$  direction vibration of the planet occurs and these modes are named single planet mode.

Based on free vibration analysis, the time response analysis of the drive system to electric excitation is given by Eq. (19). The dynamic time responses are shown in Fig. 3. Here, the exciting frequency  $\omega_e = 50$  rad/s and the modal damping is 3 percent. Fig. 3(a) shows results under condition that only the first phase exciting voltage is considered, Fig. 3(b) is for the second phase exciting voltage, Fig. 3(c) is for the third phase exciting voltage, and Fig. 3(d) shows results under condition that three phase exciting voltages are considered. In Fig. 3, the curves 1 and 2 show dynamic displacements  $\Delta u_i$  and  $\Delta z_i$  of the planet, respectively, and the curve 3 shows dynamic displacement  $\Delta u_r$  of the rotor. From Fig. 3, it is known:

(1) Only for the three rotational modes (corresponding to  $\omega_1 = 303$  rad/s,  $\omega_4 = 584$  rad/s and  $\omega_7 = 1919$  rad/s), the forced responses of the system to electric excitations occur. As vibrations of all the planets are identical for rotational mode, only the results about one planet are presented.

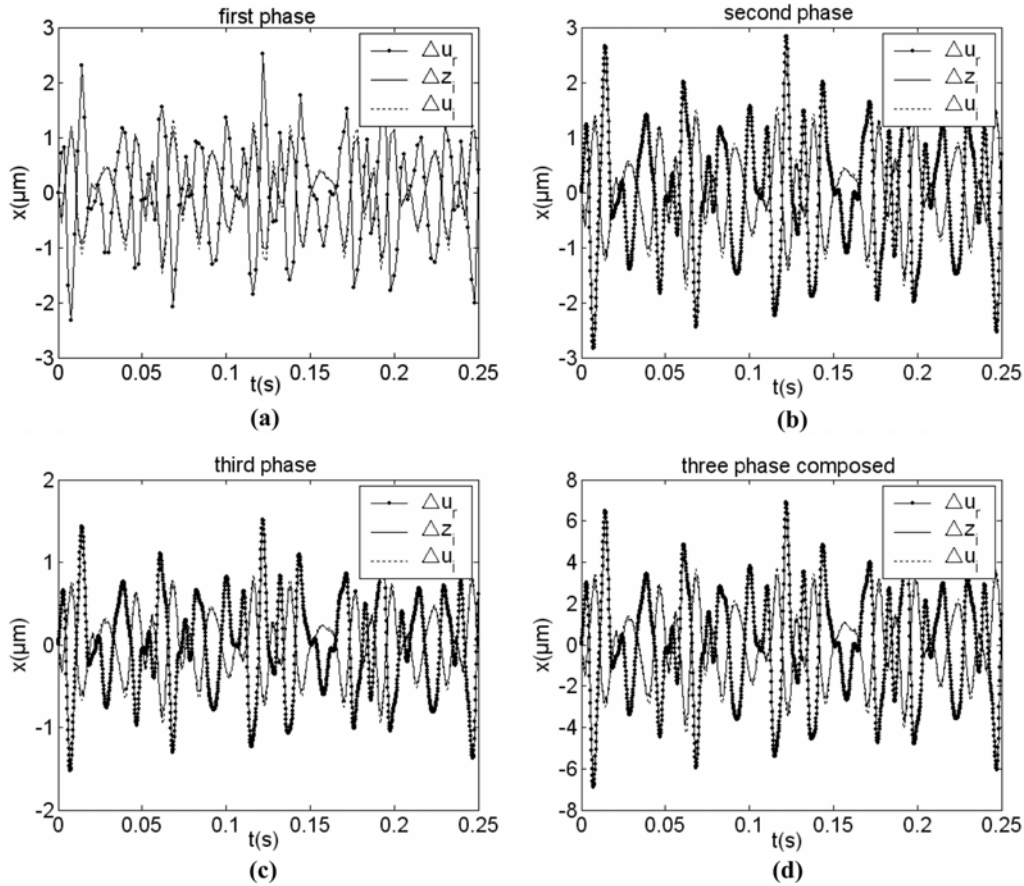


Fig. 3 Time response of the drive system to electric excitations; (a) The first phase electric excitation, (b) The second phase electric excitation, (c) The third phase electric excitation, (d) Three phase electric excitations

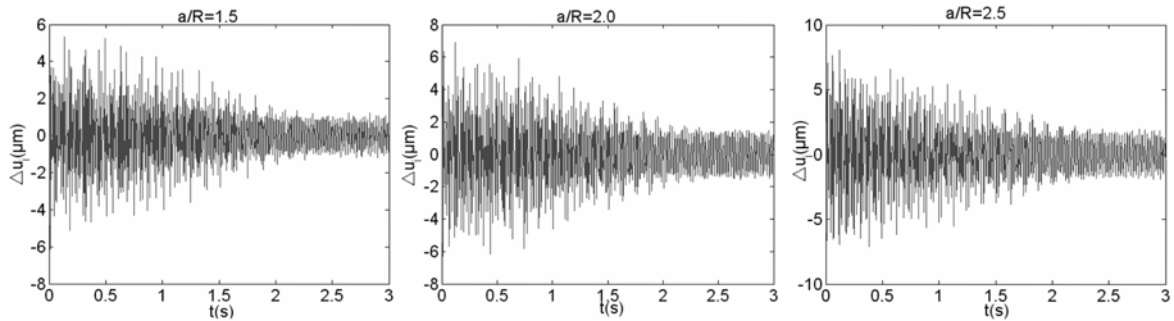
(2) The vibrating amplitude of the displacement  $\Delta u_r$  is larger than those of the displacements  $\Delta u_i$  and  $\Delta z_i$ , and the vibrating amplitude of the displacements  $\Delta u_i$  is near to  $\Delta z_i$ . It is because the exciting frequency ( $\omega_e = 50$  rad/s) is low and the rotational vibration of the rotor is principal.

(3) When only the second phase exciting voltage is considered, the vibrating magnitudes of the displacements  $\Delta u_r$ ,  $\Delta u_i$  and  $\Delta z_i$  are all large. And when only the third phase exciting voltage is considered, the vibrating magnitudes of the displacements  $\Delta u_r$ ,  $\Delta u_i$  and  $\Delta z_i$  are all small. It is because three phase coils on the worm are arranged asymmetrically.

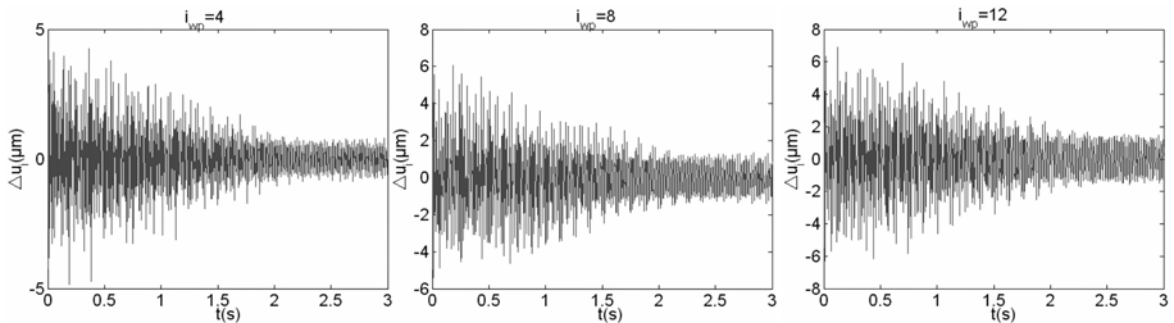
(4) When three phase exciting voltages are all considered, the vibrating magnitudes of the displacements  $\Delta u_r$ ,  $\Delta u_i$  and  $\Delta z_i$  are all larger than those when only one phase exciting voltage is considered. The total dynamic responses are decided by three phase exciting voltages, exciting frequency and natural frequencies of the drive system.

(5) Electric excitations cause the initial vibrations and the forced vibrations. The initial vibrations vanish quickly and only the forced responses are remained.

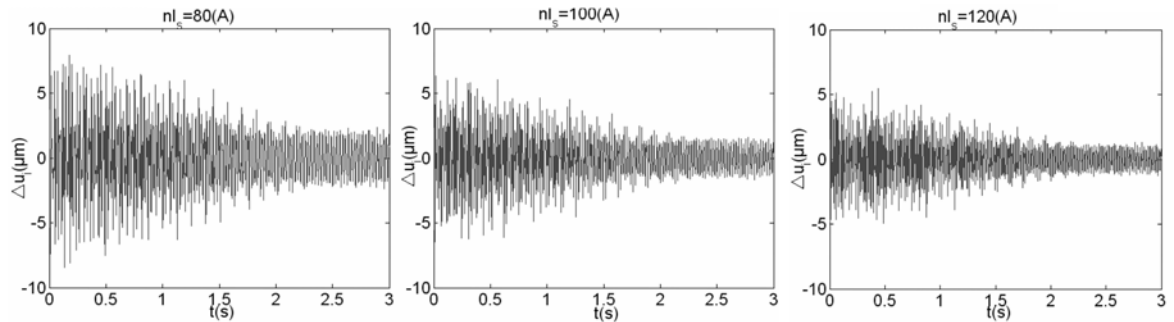
The changes of the time responses along with main parameters of the drive system are shown in Fig. 4. From Fig. 4, the following observations are worth noticing:



(a) Changes of the time response along with  $a/R$



(b) Changes of the dynamic response along with  $i_{wp}$



(c) Changes of the dynamic response along with  $nI_s$

Fig. 4 Changes of the time response along with drive parameters

- (1) As the ratio  $a/R$  increases, the displacement  $\Delta u_i$  increases obviously. It is because mesh stiffness of the drive system decreases obviously with increasing the ratio  $a/R$ .
- (2) As the ratio  $i_{wp}$  increases, the displacement  $\Delta u_i$  increases. It is because mesh stiffness of the drive system decreases with increasing the ratio  $i_{wp}$  as well.
- (3) As the current parameter  $nI_s$  increases (here  $n$  is turn number of coils), the displacement  $\Delta u_i$  decreases obviously. It is because mesh stiffness of the drive system increases with increasing the ratio parameter  $nI_s$ .
- (4) Changes of displacements  $\Delta u_r$  and  $\Delta z_i$  along with above parameters are similar to ones of displacement  $\Delta u_i$ . Here, they are not presented.

4.2 Frequency response

Eqs. (20) and (21) are used for the frequency response analysis of the drive system to electric excitation. The dynamic frequency responses are shown in Fig. 5. In Fig. 5, the curve 1 is for

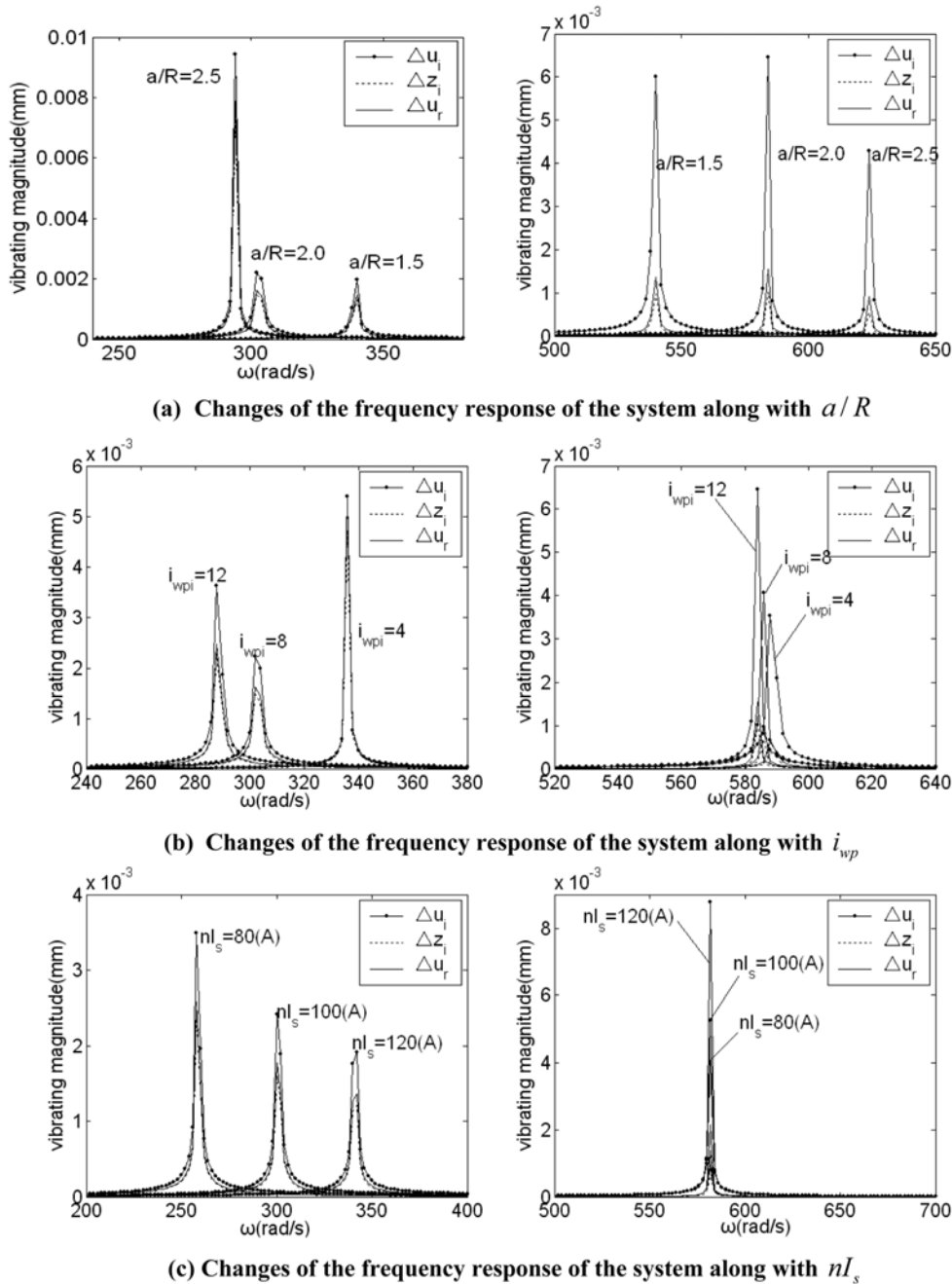


Fig. 5 Influences of parameters on frequency response of the system to load excitations

vibrating amplitude of the dynamic displacement  $\Delta u_i$ , the curve 2 for the dynamic displacement  $\Delta z_i$ , and the curve 3 for the dynamic displacement  $\Delta u_r$ . From Fig. 5, the following observations are worth noticing:

(1) As the ratio  $a/R$  increases, the natural frequencies decrease and the resonance peaks drop at first, they reach their minimum at  $a/R = 2$ , and then grow at lower frequency (below 380 rad/s). At higher frequency (above 380 rad/s and below 700 rad/s), as the ratio  $a/R$  increases, the natural frequencies increase, and the resonance peaks grow at first, they reach their maximum at  $a/R = 2$ , and then drop. These results are mainly decided by changes of the mesh stiffness and the equivalent exciting force along with ratio  $a/R$ . At lower frequency (below 380 rad/s), the mesh stiffness decreases with increasing the ratio  $a/R$  and the natural frequencies decrease. However, the equivalent exciting force also decreases with increasing the ratio  $a/R$ . At  $a/R = 2$ , the decrease of the exciting force is principal and the vibrating amplitudes decrease. At  $a/R = 2.5$ , the decrease of the mesh stiffness is principal and the vibrating amplitudes increase obviously. At higher frequency (above 380 rad/s and below 700 rad/s), the mesh stiffness and the natural frequencies increases with increasing the ratio  $a/R$ . Changes of the vibrating amplitudes along with the ratio  $a/R$  are also influenced by changes of the mesh stiffness and the equivalent exciting force.

(2) As the ratio  $i_{wp}$  increases, the natural frequencies decrease and the resonance peaks drop at first, they reach their minimum at  $i_{wp} = 8$ , and then grow at lower frequency (below 380 rad/s). At higher frequency (above 380 rad/s and below 700 rad/s), as the ratio  $i_{wp}$  increases, the natural frequencies decrease slightly and the resonance peaks grow obviously. These results are decided by changes of the mesh stiffness and the equivalent exciting force along with ratio  $i_{wp}$  as well.

The parameter  $i_{wp}$  is the speed ratio between the worm and the planet. It equals ratio of the planet tooth number to the pole pair number of the worm coils. As the pole pair number of the worm coils is generally taken as 1 or 2, and the planet tooth number is generally taken 6-12 (it is limited by the size of the planet), the general value of the speed ratio  $i_{wp}$  ranges 3-12. Hence, three different ratios 4, 8 and 12 of the parameter  $i_{wp}$  are used.

The change of the ratio  $i_{wp}$  will influence magnetic mesh stiffness between the worm and the planet and the equivalent exciting force caused by the voltage fluctuation. As the ratio  $i_{wp}$  increases, both magnetic mesh stiffness between the worm and the planet and the equivalent exciting force decrease. The results in Fig. 5(b) are caused by the changes of the mesh stiffness and the equivalent exciting force.

In the higher frequency range, changes of the equivalent exciting force along with the ratio  $i_{wp}$  are not obvious and the vibrating amplitudes are mainly influenced by stiffness changes. Therefore, as the ratio  $i_{wp}$  increases the vibrating amplitudes increases. However, in the lower frequency range, the changes of the equivalent exciting force along with the ratio  $i_{wp}$  are obvious and the vibrating amplitudes are decided by stiffness and exciting force changes. The influence of the exciting force changes is larger than that of the stiffness changes. Therefore, as the ratio  $i_{wp}$  increases the vibrating amplitudes decreases. After  $i_{wp} \geq 8$ , the decrease of the exciting force along with increasing ratio  $i_{wp}$  becomes slow. So, the amplitude at  $i_{wp} = 12$  is smaller than that at  $i_{wp} = 4$ , but larger than that at  $i_{wp} = 8$ .

(3) As the parameter  $nI_s$  increases, the natural frequencies increase and the resonance peaks decrease at lower frequency (below 380 rad/s). At higher frequency (above 380 rad/s and below 700 rad/s), as  $nI_s$  increases, the natural frequencies nearly do not changes and the resonance peaks grow obviously. These results are decided by changes of the mesh stiffness and the equivalent exciting force along with the parameter  $nI_s$  as well. At lower frequency (below 380 rad/s), the mesh stiffness

and the equivalent exciting force increase along with increasing  $nI_s$ , but the increase of the stiffness is principal. At higher frequency (above 380 rad/s and below 700 rad/s), the mesh stiffness is not nearly influenced by  $nI_s$  and the equivalent exciting force increase along with increasing  $nI_s$ .

## 5. Conclusions

In this paper, the equivalent exciting force caused by electric excitation is derived. The analytical equations of the time responses for the drive system to electric excitations are obtained. The transfer function of the drive system is given. These equations are used for analysis of the time and frequency response for the drive system to the electric excitation. It is known that electric excitations can cause forced response of the drive system, and the total responses are decided by three phase exciting voltages, exciting frequency and natural frequencies of the drive system, the drive parameters have obvious influence on the time and frequency responses.

## Acknowledgements

This project is supported by National Natural Science Foundation of China (No50375132).

## References

- Atallah, K., Calverley, S.D. and Howe, D. (2004), "Design, analysis and realisation of a high-performance magnetic gear", *IEE Proc.: Electric Power Applications*, **151**(2), March, 135-143.
- Barth, Oliver (2000), "Harmonic piezodrives-miniaturized servo motor", *Mechatronics*, **10**, 545-554.
- Da Lio, M., Nista, A. and Viola, F. (1994), "Electromagnetic harmonic motor with continuous control of position and torque", *Proc. of the 27th Applications in the Transportation Industries*: Archen, German, Aug., 487-491.
- Kuehnle, M.R. (1966), Toroidgetriebe. Urkunde uber die Erteilung des deutschen Patents, 1301682.
- Kuehnle, M.R. (1988), "Toroidal drive system and method of assembling same", United States Patent, 5784923.
- Kuehnle, M.R. (1999), "Toroidal transmission and method and apparatus for making and assembling same", United States. Patent, 5863273.
- Kuehnle, M.R., Peeken, H., Troeder, H. and Cerniak, S. (1981), "The toroidal drive", *Mech. Eng.*, **32**(2), 32-39.
- Okano, Makoto, Tsurumoto, Katsuo, Togo, Shinichi, Tamada, Noriharu, and Fuchino, Shuichiro (2002), "Characteristics of the magnetic gear using a bulk high-Tc superconductor", *IEEE T. Appl. Supercon.*, **12**(1), 979-983.
- Rasmussen, P.O., Andersen, T.O., Joergensen, F.T. and Nielsen, O. (2003), "Development of a high performance magnetic gear", *Conf. Record - IAS Annual Meeting (IEEE Industry Applications Society)*, **3**, 1696-1702.
- Shang, Zhenguo and You, Zhuping (1997), "Control system for magnetic type harmonic gear drive", *Zhizao Jishu Yu Jichuang/Manuf. Technol. Mach. Tool (in Chinese)*, **2**, 7-10.
- Xu, L. (2004), "Efficiency for toroidal drive", *Proc. of the 11th World Congress in Mechanism and Machine Science*, Tianjin, China, April, 737-740.
- Xu, L. and Huang, J. (2005), "Torques for electromechanical integrating toroidal drive", *Proc. of the I MECH E Part C J. Mech. Eng. Sci.*, **219**(8), 801-811.
- Xu, L. and Huang, Z. (2003), "Contact stresses for toroidal drive", *J. Mech. Design -T. ASME*, **125**(3), 165-168.
- Xu, L., Huang, Z. and Yulin Yang (2004), "Mesh theory for toroidal drive", *J. Mech. Design -T. ASME*, **126**(3), 551-557.
- Yao, L., Dai, J.S. and Li, H. (2004), "Mathematical modelling and manufacturing of the internal Toroidal tooth

- profile”, *J. Mech. Eng. Sci., Proc., IMechE, Part C*, **218**(9), 1043-1051.
- Yao, L., Dai, J.S., Wei, G. and Li, H. (2005), “Geometric modeling and meshing characteristics of the toroidal drive”, *J. Mech. Design -T. ASME*, **127**(5), 988-996.
- Yao, L., Dai, J.S., Wei, G. and Li, H. (2006), “Comparative analysis of meshing characteristics with respect to different meshing rollers of the toroidal drive”, *Mech. Mach. Theory*, **41**(7), 586-604.
- Yao, L., Dai, J.S., Wei, G. and Li, H. (2006), “Error analysis and compensation for meshing contact of toroidal drives”, *J. Mech. Design -T. ASME*, **128**(3), 1000-1010.
- Yao, L., Wei, G. and Lan, Z. (2005), “Comparative study on machining the internal stationary Toroidal Gear”, *Key Eng. Mater., Adv. Abrasive Technol.*, **291-292**, 483-488.

## Notation

$u_i$	: rotating displacement of the planet $i$
$u_r$	: rotating displacement of the rotor
$r_i$	: rolling circle radius for planet $i$
$r_r$	: radius of the circle passing through planet centers for the rotor
$\theta_i$	: rotation of planet $i$
$\theta_r$	: rotation of rotor
$m$	: planet number
$\mathbf{q}_j$	: displacement vector for planet $j$
$\mathbf{m}_j$	: mass matrix for planet $j$
$J_j$	: polar mass moment of inertia for planet $j$
$J_r$	: polar mass moment of inertia for rotor
$m_j$	: mass of planet $j$
$M_r$	: equivalent mass of rotor
$\gamma_{wpi}$	: lead angle at contact point between planet- $i$ and worm
$\gamma_{spi}$	: lead angle at contact point between planet- $i$ and stator
$a$	: center distance between worm and planet
$R$	: reference circle radius of planet
$i_{wp}$	: speed ratio between planet and worm
$i_{sp}$	: speed ratio between planet and stator
$\mathbf{X}$	: displacement vector
$\mathbf{F}$	: load vector
$\mathbf{M}$	: mass matrix
$\mathbf{C}$	: damp matrix
$\mathbf{K}$	: stiffness matrix
$\phi_v$	: face width angle of the worm
$\phi_i$	: phase angle of the phase- $i$ voltage
$n_p$	: phase number of the worm coils
$p$	: number of the pole-pairs
$z_1$	: tooth number of planet
$L_{ii}$	: self-inductance of the coils
$L_{ij}$	: mutual-inductance of the coils
$L_0$	: average inductance
$L_1$	: the first order harmonic component of the inductance
$\lambda_i$	: magnetic linkage of the coils
$I_i$	: current of the $i$ th phase worm coils
$W$	: magnetic energy storage of the electric system
$F$	: electromagnetic force between magnet poles
$d\zeta$	: relative displacement between magnet poles
$d\theta$	: relative rotating angle between magnet poles

$F_{wp}$	: electromechanical coupled force between a tooth of the planet- $i$ and worm
$\theta_0$	: static relative rotating angle between planet and worm
$\delta I_i$	: current increment of the $i$ th phase coils
$F_e(t)$	: equivalent electric exciting force
$\Delta F_{wp}$	: electromechanical force increment between a tooth of the planet- $i$ and worm
$\delta\theta$	: dynamic relative rotating angle between planet and worm
$\bar{\mathbf{F}}$	: static load vector
$\Delta\mathbf{F}$	: dynamic load vector
$\bar{\mathbf{X}}$	: static displacement vector
$\Delta\mathbf{X}$	: dynamic displacement vector
$\Delta\mathbf{v}(t)$	: electric voltage excitation vector
$v$	: amplitude of the exciting voltage
$\omega_e$	: exciting frequency
$r_\Omega$	: resistance of each phase worm coils
$I$	: effective value of the current
$F_{e1}(t)$	: equivalent exciting force under the first phase voltage excitation
$F_{e2}(t)$	: equivalent exciting force under the second phase voltage excitation
$F_{e3}(t)$	: equivalent exciting force under the third phase voltage excitation
$\mathbf{M}_r$	: diagonal mass matrix
$\mathbf{C}_r$	: diagonal damping matrix
$\mathbf{K}_r$	: diagonal stiffness matrix
$\Delta\mathbf{F}_r$	: transmitted exciting force vector
$\Delta\mathbf{X}_r$	: transmitted dynamic displacement vector
$\mathbf{A}_r$	: mode matrix
$\omega_r$	: the $r$ th natural frequency of mechanical system
$\gamma_r$	: the $r$ th relative damping coefficient
$M_r$	: the $r$ th transmitted mass
$K_r$	: the $r$ th transmitted stiffness
$x_{Nr}$	: time response of the $r$ th regular coordinate
$\Delta F_{Nr}(t)$	: the $r$ th regular exciting force
$\Delta F_{Nr}$	: magnitude of the $r$ th regular exciting force
$n$	: turn number of coils
$A$	: mode matrix